Experiment and modelling of birefringent flows using commercial CFD code

R.A. Tomlinson *, D. Pugh, S.B.M. Beck

Department of Mechanical Engineering, The University of Sheffield, Mappin Street, Sheffield S1 3JD, UK

Abstract

It is well-known that certain fluids are birefringent and when flows are viewed in polarised light interference fringes are observed. The fringes are caused by a phase shift in the light passing through the fluid and are proportional to the integral of the maximum shear strains in the fluid. In order to understand what is happening within the three dimensional flow and overcome the difficulties due to this integration, additional computational or experimental information is needed.

In this work, a commercially available computer code (Fluent) is used for the first time to model the flows. The flow data are then exported to a spreadsheet where the shear rates are integrated across the field and then banded for graphical output. The results from this are then compared to results generated from birefringent flow experiments and the agreement is found to be good since the modelled fringes show the same patterns as those in the experiment. This novel use of computational and experimental techniques together will allow quantitative analysis of three-dimensional flows in the future.

Currently, there are still a lot of empirical variables involved in fitting the computational fringes to the experiment, but the results of this preliminary study show that this is a promising approach to this type of problem.
© 2006 Elsevier Inc. All rights reserved.

Keywords: Birefringent flows; Computer modelling; Experiments; Shear rate

1. Introduction

The photoelastic effect is that property of transparent materials which causes them to become birefringent or doubly refracting when deformed. In their free state, materials such as glass, plastics and fluids are isotropic to the passage of light; light traversing them is affected only by the normal elementary laws of optics. When deformed however, these materials behave like most transparent crystals, in that they have distinct optical axes and transmit light with different velocities along the planes of principal strain. When a ray of light passes through a birefringent material under strain, it is split into two components appropriate to the principal strains at any point; each ray then passes through the material at a velocity which is proportional to the magnitude of the principal strain with which it is associated, i.e. the material behaves as if it has two refractive indices, hence the term birefringent. When the light exiting the material is viewed through a polarising plate, interference fringes can be observed. These fringes are caused by the phase shift in the light that has passed through the material and are proportional to the maximum shear strain in the material. Using birefringence to study strain in solid materials is well-established and is termed *photoelasticity*. The practical use of birefringence effects in fluids is still in its infancy but it has already been used by Sun et al. (1999) for examining blood flow in models of cardiovascular systems. As polymer melts are themselves birefringent, this is one of the prime applications of the technique as exemplified by Martyn et al. (2000).

Maxwell (1872) and Mach (1873) first observed the phenomenon of flow birefringence in the 1870s. Early

---

* Corresponding author. Fax: +44 0114 222 78890.
  E-mail address: r.a.tomlinson@sheffield.ac.uk (R.A. Tomlinson).

investigations into flow birefringence centred mainly on finding a suitable fluid that could be used and which would produce sufficient fringes. Quantitative studies of flow birefringence did not begin until the 1950s. Theories produced to explain the phenomena of flow birefringence have centred mainly around two areas:

(1) Stretching and orientation of long chain polymers.
(2) Deformation or orientation of suspended macromolecules or colloidal particles.

The fluids tested as part of this research fall into the second of these categories. Until the work of Rosenberg (1952) the accepted theory was that birefringence in fluids was due to the orientation of the molecules, but then he suggested that the birefringent effect was due to deformation of the molecules rather than their orientation. This implies that the interference fringes are related to the maximum shear stress in the fluid, τ_{max}, and not the streamlines as previously assumed. Therefore the effect is governed by the stress optical law which can be found in Dally and Riley (1991):

$$2\tau_{max} = \frac{N\lambda}{cd} \qquad (1)$$

where N is the order of the fringe observed, c is the stress optical constant, d is the length of the light path in the fluid and λ is the wavelength of the light.

This phenomenon therefore only occurs in birefringent fluids which are subject to shear stresses; the speed at which the two rays within the fluid travel is also dependent on the magnitude of these shear stresses. This means that as the stress varies within the fluid, the optical phase difference also changes. So the total birefringent effect along the light path is clearly the integral of the magnitude and direction of the shear stresses of the fluid, τ,

$$\tau = \mu\left(\frac{du}{dy}\right) \qquad (2)$$

where μ is the viscosity and du/dy is the change in velocity, perpendicular to the velocity direction.

This fact is particularly important for real, three-dimensional flow, because a shear occurs at the walls giving additional fringes due to the integrating effect. A review of integrated birefringence in both solids and fluids up to 1998 can be found in Cen et al. (1998). In order to understand what is happening within the flow and overcome this integrating effect, either additional experimental or computational techniques must be used augment the information available. Aben and Puro (1997) have investigated the use of optical tomography for 3-D flow, but this method is intensive both in terms of storage and processing requirements. Laser Doppler Anemometry (LDA) techniques have been used in conjunction with birefringence to analyse two and three-dimensional flows in non-Newtonian fluids by Davidson et al. (1993). The same pair of techniques were used by Subramanian and Picot (1996) to determine the stress optical coefficient using a convergent channel. Their flows were slow, and thus the non-Newtonian effects were very pronounced.

Various workers have use a variety of methods to model and validate birefringence. These tend to be made more difficult by the fact that most birefringent fluids tend to be non-Newtonian, adding a further layer of complexity. Grillet et al. (2000) used a hybrid experimental finite element method to simulate these flows. They looked at instabilities in lid driven cavities. However, they ignored the third-dimension in this work. The pompom method is a recent technique used to model 3-D fluid flow in polymer melts. The extended form was used by Verbeeten et al. (2004) to model this type of birefringent flow, but the authors' main concerns were related to the convergence of the solution. Clemeur et al. (2004) used the double converted form along with a Mueller Matrix method to describe the birefringent effect to allow comparison of their results with experiment.

A different approach to the modelling was published by Li et al. (2000) who used their own computational fluid dynamics (CFD) techniques to model and validate birefringence results. Other work by the group incorporates shear thinning, and is mostly concerned with the rheology of the flow.

The objective of the current research was to develop an alternative, simpler method for modelling the birefringent effect. It uses a commercial CFD code (Fluent) and converts flow fields into shear fields by post processing using a spreadsheet. By summing these calculated shears, it is possible to compare these results to experimental ones. Two different types of flows were investigated, an expanding circular jet and a cavity. The former gave a three-dimensional shear flow in the direction of the light and the latter was designed to give a two-dimensional effect. This use of a well-validated CFD code means that future research will be able to avoid the extremely time consuming task of code writing.

2. Experimental work

2.1. Optical apparatus

All the experiments in this investigation used a circular polariscope (Fig. 1). The light source was capable of producing both white and monochromatic light and was placed behind a frosted glass screen to diffuse the light and ensure the light intensity was uniform over the full
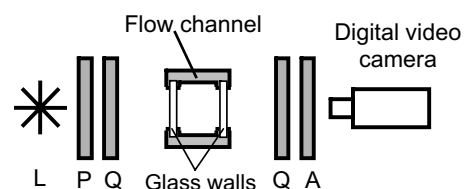

Fig. 1. Experimental arrangement of the circular polariscope, where: L = light source; P = polariser; Q = quarter wave plate; A = analyser.

field, reducing the glare. The light passed through the first polariser and a quarter wave plate, then through the flow channel under investigation, through a second quarter wave plate, and polariser (known as the analyser). The birefringent effect of the fluid was captured using a digital video camera from which individual frames could be acquired for analysis. The entire apparatus was surrounded by blackout curtains to remove the background light. This not only made the fringes easier to see but also prevented reflections from the waveplates that would cause the camera problems in focusing. Details on photoelastic analysis can be found in the excellent book by Dally and Riley (1991).

2.2. Expanding circular jet

When a relatively fast moving flow of fluid in a small pipe enters a larger volume, it forms a jet and there is high shear between the fast and slow moving fluids. This, along with a certain amount of entrainment, causes the flow to slow down and expand. This flow phenomenon is known as an expanding jet. It was decided to use this for the initial birefringent flow experiments as the high shear rates involved would maximise the fringes.

The flow channel for the expanding jet consisted of a 10 ml syringe which forced the fluid through a 1.8 mm circular hole into a 10 mm × 15 mm rectangular channel 50 mm long. The top of the channel had a Funnel attached
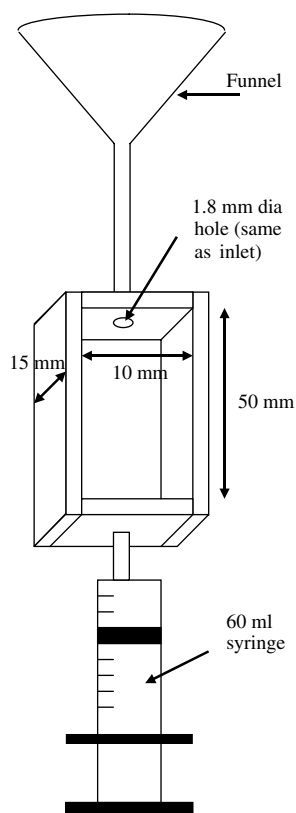

Fig. 2. Cross-sectional diagram of the cavity.

to it via a 1.8 mm hole to act as a reservoir (Fig. 2). The channel was constructed from a PMMA frame with two glass walls through which the fluid could be viewed (see Fig. 1). The glass was of negligible integrated birefringence and therefore did not affect the observed effects from the fluid. The channel was positioned between the two quarter waveplates and was orientated so the syringe forced the fluid vertically upwards. The camera was focused so that the entire channel was visible. Since part of the syringe was in the frame of the camera, the flow rate of the fluid could be calculated by taking the volume change over a number of frames, each of 0.04 s duration.

The fluid chosen for the experiment was hydroxypropyl cellulose (HPC) at 12% concentration by weight. When the fluid was propelled into the channel, it expanded rapidly in the form of a circular jet. This caused flow separation and high shear stresses within the fluid and images of the birefringent effect were recorded in both light and dark field arrangements, as shown in Fig. 3.

The rate at which the syringe needed to be depressed to produce good fringe patterns was very rapid and hence the fringes were only visible for about six frames ($\approx$0.25 s). This made the accurate calculation of the velocity of the fluid difficult, but it was approximately 10 m s^{-1}. The rapid depression rate also meant that in the dark field arrangement the light intensity suddenly increased and then decreased, reducing the quality of the pictures. The solution also had small air bubbles forced into it by the high flow rate, and the solution needed to be left to settle between runs to remove these. Ideally the fluid would be continuously pumped, but due to the viscosity of the fluid, a positive displacement pump would be needed and was not available.

Strong fringe patterns were observed in the expanding jet and in the case of the dark field arrangement in Fig. 3(b) coloured areas can clearly be seen and these were used to analyse the order of the fringes for comparison with the computational model. Although the jet experiment produced strong fringe patterns, the analysis of these fringes alone is difficult as the nature of the flow is three-
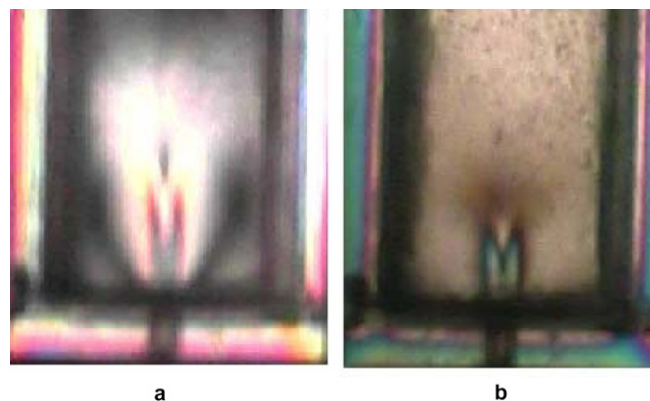

Fig. 3. Showing the birefringent fringes due to the 12% HPC acting as an expanding circular jet in (a) a light field polariscope and (b) a dark field polariscope.

dimensional and the fringes that are seen are due to the integral of the shear stresses through the sample. Hence the images in Fig. 3 do not look like a classical jet but have a bifurcated appearance. The perceived difference between the expected and actual fringe pattern is a possible reason why commercial CFD codes have not been used previously in this field.

The concentration of the HPC was lowered in 1% increments to 6%. Here fringes were still visible but of lower order than before. The maximum fringe order observed varied with the concentration of the solution reducing from a maximum of 1.5 fringes to 0.5 fringes with the 12% and 6% concentrations, respectively. This observation may be explained by the fact that the viscosity and therefore shear stress reduce with concentration, thus lowering the fringe order.

2.3. Two-dimensional flow in a cavity

A second channel was designed to approximate two-dimensional flow as shown in Fig. 4. This channel had a rectangular cross-section with a large thickness to width ratio which ensured that the path of the light would be relatively long without the volume of the channel becoming too large. This was important, as the length of the light path, d, directly affects the number of fringes produced (see Eq. (1)). A backward facing step was included in the channel to produce the high shear stresses. The fluid was forced into the channel from a 60 ml syringe with a short length of copper pipe inserted into the end of it, via 6 mm tubing into a 75 mm long duct 3 mm high and 18 mm thick. This allowed the velocity profile to become fully developed. The fluid then passed over a backward facing step 8 mm in height into a chamber 50 mm long. The duct then reduced back to the same dimensions as the inlet and another 6 mm tube was used at the outlet. This tube led to a vertical funnel which was used both as a reservoir and a filling mechanism. The sudden expansion of the fluid after the step caused flow separation and hence high shear stresses in the fluid. The shear stresses and thus the fringes in the birefringent fluid occurred directly after the step, so the camera was focussed on this area.

This channel was also constructed with glass walls either side which were held in place by grooves in a PMMA frame. The end sections of the channel were secured by the use of screws. This channel was placed between the two quarter waveplates (Fig. 1) so that the glass sides were parallel to them. The syringe was clamped vertically with
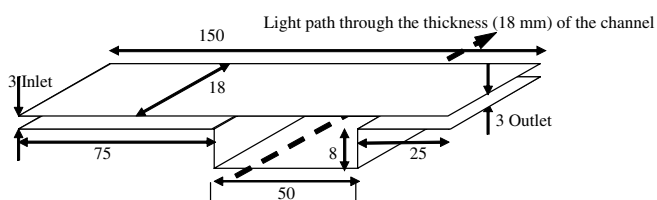

Fig. 5. Showing the fringe pattern observed the cavity using 7% concentration of HPC in a dark field polariscope.

the outlet facing downwards which helped to prevent air bubbles entering the channel during the experiments as the air in the syringe would automatically rise to the top.

The initial experiments for flow in the cavity used a 12% concentration of HPC. This was then reduced in 1% increments down to 7% (Fig. 5 shows the fringes observed in the channel with a concentration of 7%). For each concentration the flow rate and image of the birefringent fringes were recorded. The flow rate was calculated by recording on the soundtrack of the video camera when the fluid had reached certain levels. High concentrations of HPC, with high fluid viscosity, produced low fluid flow rates and could only be timed over 5–20 ml. Once the concentration reached 7%, the viscosity had dropped sufficiently for the fluid to be timed over the entire 60 cm^3 volume of the syringe.

It had been expected that due to the higher flow rates at lower viscosities, the fringe order would decrease with decreasing concentration, in a similar way to the observations in the expanding jet. However it was noticed that the fringe order was increasing rather than decreasing. The HPC was diluted further in increments of 0.5% down to 4%.

3. Computational modelling

All the modelling work to produce the velocity fields used the CFD package FLUENT4. The computational grid models were created in Pre-BFC and after convergence, velocity components were imported into a spreadsheet. The velocity boundary conditions and fluid properties were obtained from the experimental work described above. Once in the spreadsheet the velocities were transformed from u, v and w components into velocity magnitudes using Pythagoras' theorem.

The shear stress, τ, at each point requires the differential of the velocity magnitude and these were found for every node using upwind differencing in the z direction (in the direction of the light path—see Fig. 4). It is appreciated that any method of producing the partial differentials could be used

$$\frac{\partial u}{\partial y} \approx \frac{u_i - u_{i-1}}{y_i - y_{i-1}} \tag{3}$$

Fig. 4. Cross-sectional diagram of the cavity.

where i is the element and $i - 1$ is the previous element with respect to the light path.

A two-dimensional projection of these results was produced by summing these results in the z direction which gave values proportional to the optical phase shifts. A surface plot of these was produced, and when correctly banded, could be compared with the experimental fringe pattern.

To make the CFD calculations easier, the fluid was treated as Newtonian. It was also assumed that flow birefringence obeys the stress optic law, Eq. (1) and that indices of refraction that are related to the shear stress are the sole cause of the birefringent effect.

3.1. Modelling of expanding jet

The domain for the model of the expanding jet was $20 \times 60 \times 12$ cells. In order to reduce the computational time, only one quarter of the channel was modelled and symmetry cells were used in both directions perpendicular to the flow. To increase the information in the inlet, the concentration of cells was doubled in the inlet half of the channel so that there were 40 cells were in the first half and only 20 in the second half.

Two flow situations were modelled, using 6% and 12% solutions of HPC. As can be seen in Fig. 6, after processing the data, the 6% solution gave a good agreement with the experimental observations. In this figure, the experimental and computational data are shown as mirror images on either side of the centre line with the flow going from left to right. The 12% solution of HPC however produced inferior results, as the modelled fringes produced did not appear to spread out at the entrance to the channel. This was thought to be due to the non-Newtonian nature of the fluid as was borne out from the experimental observations that fringes were "frozen" into the fluid at the end of the step experiments. Although probably present at higher concentrations, this effect was first noticed at 10% concentration. At the base of the step, a permanent fringe was observed after drawing the fluid into the syringe (Fig. 7). Very faint fringes were also noticed after experiments

Fig. 6. Experimental and Computational fringe patterns from the expanding jet experiment using 6% HPC.

Fig. 7. Stress frozen fringe in the cavity using 10% HPC.
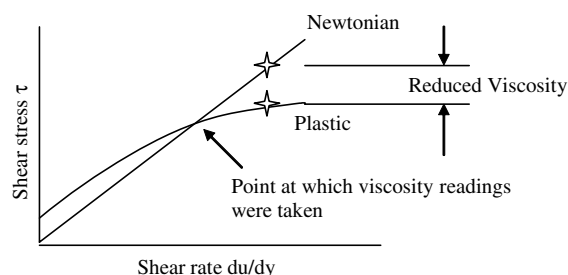

Fig. 8. Expected (Newtonian) and real (plastic) relationship.

where stronger fringes had been present during flow. Unfortunately these fringes were too faint for the camera to pick up. These stress frozen fringes indicate that the solution is capable of withstanding a shear force without deforming, which is evidently a non-Newtonian feature of the fluid.[1] An additional issue of this non-Newtonian flow was that the Reynolds number was not entirely correct. The initial assumption for the computational model was that the fluid was Newtonian with a viscosity measured at a relatively low rate of shear. The actual viscosity was lower than this value, as shown in Fig. 8. It was therefore decided to repeat the computational model with the viscosity lowered from $1.6 \text{ kg m}^{-1} \text{ s}^{-1}$ to $0.74 \text{ kg m}^{-1} \text{ s}^{-1}$. At this value, the fringe pattern of the jet was seen to bifurcate as observed during the experiments (Fig. 9). This value was used for all the analysis using 12% HPC solutions. As the computational model is seen to agree well with the experimental results, this implies that the approach taken to process the results is an acceptable one for these preliminary studies.

3.2. Modelling of the cavity

The grid for the cavity consisted of $100 \times 11 \times 13$ cells. As the channel had a single line of symmetry down the centre in the direction of flow this was mimicked in the computational grid by placing a surface of symmetry cells in the centre of the channel. This helped to reduce the compu-
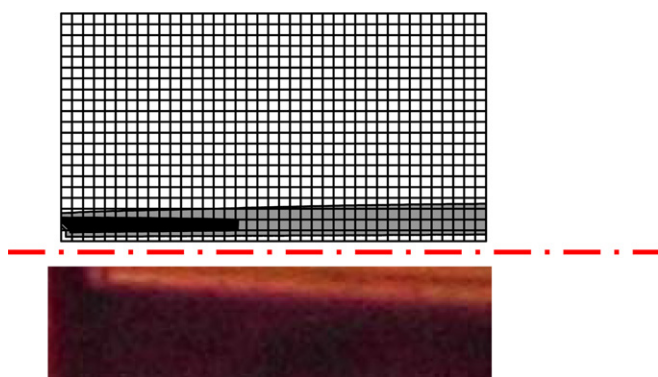

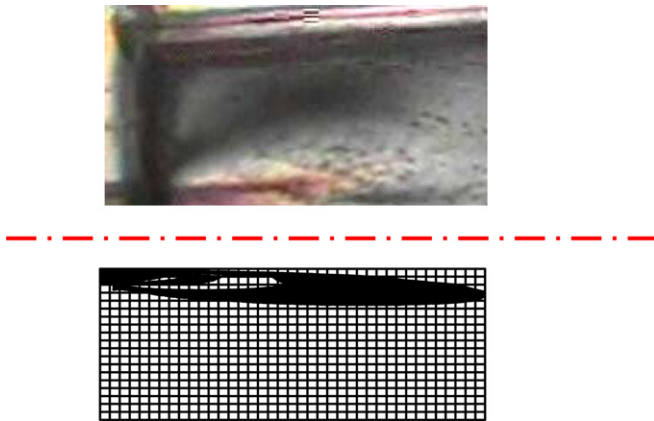[1] Establishing the non-Newtonian stress deformation law for this fluid was a task beyond the scope of the present study.

Fig. 9. Expanding jet: experimental fringe data for 12% HPC and computational fringe data using a viscosity of 0.74 kg m^{-1} s^{-1}.

tation time as well as the amount of data that needed processing. To improve the data produced by FLUENT4 the number of cells was increased for the expansion, and also in the inlet duct to ensure the flow was fully developed. Care needed to be taken at this stage as weighting of the cells incorrectly could give poor results and cause problems in the analysis. Refinement of the grid was considered in the z direction around the centre of the channel for the inlet and outlet but this was not done, as it would have caused difficulties with the differencing due to the variation in the grid size.

The computation was carried out with 5% and 10% concentrations of HPC. Once again, a correction was made to
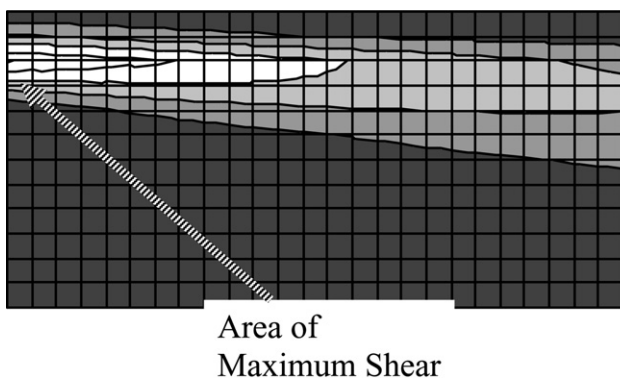

Fig. 10. Banded FLUENT4 data used to predict fringe patterns for 5% HPC and experimental results for 5% HPC.
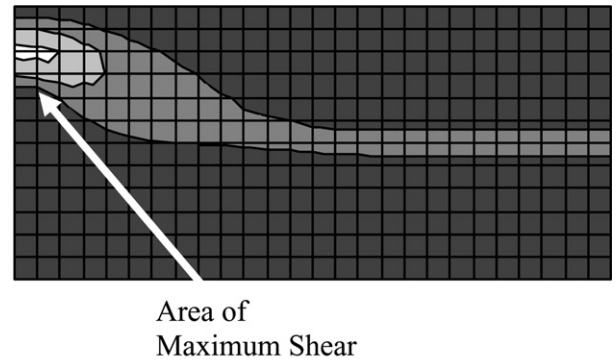

Fig. 11. Banded FLUENT4 data used to predict fringe patterns for 10% HPC.

account for the effective viscosity for the higher concentration. The fringe patterns have been banded to approximate the fringes observed experimentally and are shown, along with the equivalent experimental results in Figs. 10 (5% concentration) and 11 (10% concentration). The flow in this case goes from left to right. Although these data are not as clear as those from the expanding jet, a close resemblance can be seen in the fringe patterns. This figure shows that that the computational results can correctly predict the area of greatest shear and hence highest fringe order.

This is particularly clear when one examines the first, white, fringe from the experiment. In the case of the 5% concentration, the flow goes parallel to the top, and the maximum shear occurs as the high speed jet goes over the step which is shown in Fig. 10. The same comparison can be applied to the 10% results, except in this case the areas go down from the step at about 35° from horizontal. This is because the greater viscosity will cause the jet to become attached to the wall.

4. Discussion

The aims of this work were to show that the birefringent analysis could be applied successfully to fluid flow and that it was possible to use minor modifications of commercially available CFD software to model the fields which had been produced experimentally. In both of the geometries tested, the simple approach taken by the authors has produced acceptable results for both of these aims.

It has been shown that after processing, the salient features of both the two and three-dimensional flow experiments can be identified and explained. This is particularly

so in the case of the expanding jet where the fringes do not actually appear as expected due to the integral effect of the birefringence through the channel which gives the appearance of the flow splitting into two jets. That the modelling shows the same effect, both supports the validity of the modelling method and explains the experimental result.

Although the fringes at high concentrations are clearly visible, more fringes would be desirable. As the flow rate is close to transition to turbulent, higher flow rates are impossible as the linear birefringent effect only works in laminar flow; an increased cross-section of the flow channel would be a good method of achieving this.

The non-Newtonian nature of the fluid has been noted and to a certain extent accounted for by linearising its value at the operating condition. From the data obtained using the expanding jet and CFD, at a flow rate of $10 \, \text{m s}^{-1}$ and 12% concentrations the viscosity was found to be out by a factor of two. To obtain more correct results, a full shear rate against viscosity calibration of the fluid and also the use of the non-Newtonian flow model in FLUENT would have to be implemented.

In this work, the contribution of the shear stresses lying in the plane of the light ray was considered to be equal to that of the shear stresses perpendicular to it. This is unlikely actually to be the case and investigation into this area should be considered.

Other methods of increasing the order of the fringes produced could be examined for further investigations. Alternative solvents for HPC could be used to improve the fringes as achieved by Shtennikova and Kolbina (1995). Another method is to use partial mirrors to increase the fringe order. These work by reflecting the light back through the channel a number of times, increasing the path length of the light.

It is fully appreciated that the work shown here is still in its early stages. For example, the viscosity and fringe constants required to make the experiment and theory agree have to be chosen by the operator. Undoubtedly these could be selected on a more rigorous basis. The fluid should also be optically calibrated to enable the bands to be automatically selected. Finally, it would be relatively straightforward to implement both the non-Newtonian flow and shear rate calculations directly within the latest versions of many CFD packages, making processing the results a far easier task.

5. Conclusions

This work has shown that the use of hydroxypropyl cellulose (HPC) in investigating flow birefringence produces results that can lead to quantitative analysis of the flow fields. It also illustrates that increased flow rates have a marked effect on the fringe order.

The cavity experiments combined with CFD of the same geometry show that calibration of the fringe data from HPC is possible. The agreement between the experimental and computational results illustrates that what is happening in the flow is understood, making the two-dimensional calibration possible.

The expanding jet used has demonstrated that three-dimensional analysis of flow using flow birefringence is possible even though the results from the experiment may not appear to show the expected result. In this case computational analysis can be also used to calibrate the fluid optically. To analyse this form of flow from the birefringence results, more work is required and techniques such as tomographic analysis would be needed.

These results present a simple way forward in the modelling of birefringent flows as standard CFD codes can be used to extract flow fields which can then easily be integrated and scaled. Overall the method shows great promise and, as it is a full field method where time varying flow phenomena can be analysed, it will provide a valuable element in the fluid mechanic's toolbox.

References

Aben, H., Puro, A., 1997. Photoelastic tomography for three-dimensional flow birefringence studies. Inverse Problems 13, 215–221.
Cen, M., Hickman, L.J., Tomlinson, R.A., Patterson, E.A., 1998. Integrated birefringence applied to solids and fluids—a review. In: Proceedings of 11th International Conference on Experimental Mechanics, Oxford, August 1998, pp. 507–512.
Clemeur, N., Rutgers, R.P.G., Debbaut, B., 2004. Numerical evaluation of three-dimensional effects in planar flow birefringence. Journal of Non-Newtonian Fluid Mechanics 123, 105–120.
Dally, J.W., Riley, W.F., 1991. Experimental Stress Analysis. McGraw-Hill, Inc.
Davidson, D.L., Graessley, W.W., Schowalter, W.R., 1993. Velocity and stress fields of polymeric liquids flowing in a periodically constricted channel. 1. Experimental methods and straight channel validations. Journal of Non-Newtonian Fluid Mechanics 49 (2–3), 317–344.
Grillet, A.M., Shaqfeh, E.S.G., Khomami, B., 2000. Observations of elastic instabilities in lid-driven cavity flow. Journal of Non-Newtonian Fluid Mechanics 94 (1), 15–35.
Li, J.M., Burghardt, W.R., Yang, B., Khomami, B., 2000. Birefringence and computational studies of a polystyrene Boger fluid in axisymmetric stagnation flow. Journal of Non-Newtonian Fluid Mechanics 91 (2–3), 189–220.
Mach, E., 1873. Optische-akustische Versuche. Clava, Prague.
Martyn, M.T., Groves, D.J., Coates, P.D., 2000. In process measurement of apparent extensional viscosity of low density polyethylene melts using flow visualisation. Plastics Rubber and Composites 29 (1), 14–22.
Maxwell, J.C., 1872. Double refraction of viscous fluid motion. Proceedings of the Royal Society of London Series A 22, 46.
Rosenberg, B., 1952. Navy Dept., David W. Taylor Model Basin Report No. 617.
Shtennikova, I.N., Kolbina, G.F., 1995. Flow birefringence of hydroxypropylcelluclose molecules in aqueous and organic solvents. Vysokomolekulyarnye Soyedineniya Seriya A and Seriya B 37 (8), 1324.
Subramanian, R., Picot, J.J.C., 1996. A rheo-optical analysis of converging wedge flow for estimation of stress-optical coefficient. Polymer Engineering and Science 36 (9), 1196–1202.
Sun, Y.D., Sun, Y.F., Sun, Y., Xu, X.Y., Collins, M.W., 1999. Visualisation of dynamic flow birefringence of cardiovascular models. Optics and Laser Technology 31, 103–112.
Verbeeten, W.M.H., Peters, G.M., Baaijens, F.P.T., 2004. Numerical simulations of the planar contraction flow for a polyethylene melt using the XPP model. Journal of Non-Newtonian Fluid Mechanics 117, 73–84.